

# Numerical Simulation of Wall Treatment Effects on the Micro-Scale Combustion

R. Kamali, A. R. Binesh, and S. Hossainpour

**Abstract**—To understand working features of a micro combustor, a computer code has been developed to study combustion of hydrogen–air mixture in a series of chambers with same shape aspect ratio but various dimensions from millimeter to micrometer level. The prepared algorithm and the computer code are capable of modeling mixture effects in different fluid flows including chemical reactions, viscous and mass diffusion effects. The effect of various heat transfer conditions at chamber wall, e.g. adiabatic wall, with heat loss and heat conduction within the wall, on the combustion is analyzed. These thermal conditions have strong effects on the combustion especially when the chamber dimension goes smaller and the ratio of surface area to volume becomes larger.

Both factors, such as larger heat loss through the chamber wall and smaller chamber dimension size, may lead to the thermal quenching of micro-scale combustion. Through such systematic numerical analysis, a proper operation space for the micro-combustor is suggested, which may be used as the guideline for micro-combustor design. In addition, the results reported in this paper illustrate that the numerical simulation can be one of the most powerful and beneficial tools for the micro-combustor design, optimization and performance analysis.

**Keywords**—Numerical simulation, Micro-combustion, MEMS, CFD, Chemical reaction.

## I. INTRODUCTION

WITH the rapid progress in the mobile electrical and micro devices such as micro actuators, sensor, air vehicle and robots in the recent years, the demands on the micro-power supplier with high power density is increasing, and fabrication of such micro-devices is becoming possible. The batteries used nowadays have quite low specific energy (0.6 kJ/g for an alkaline battery and 1.2 kJ/g for a lithium battery) compared to hydrogen (140 kJ/g) and hydrocarbon fuels [2]. The promising designs due to its high power density. Development of miniaturized combustion-based power generating devices, even with a relatively inefficient conversion of hydrogen fuel to power, would result in increased lifetime and/or reduced weight of an electronic or mechanical system that currently uses batteries for power. Recent advances in the field of silicon micro-fabrication techniques and silicon-based Micro-Electro-Mechanical Systems (MEMS) have led to the possibility of a new generation of micro heat engines for power generation. Micro-combustor is one of the critical components for micro-power system using hydrogen and hydrocarbon fuels as an energy source. Several types of

micro-combustor and chemical reactor are currently under development [1]. However, as the size of micro-combustion chamber decreases to micron level, which is comparable to the laminar flame thickness, traditional combustion theory may not be able to explain and predict the details about the micro-combustion phenomena within the micro-combustor. In addition, the experimental method and diagnostic techniques developed for the macro-combustion facilities, becomes inapplicable for the micro-combustor due to the limitation of combustion chamber size and the complexity of the micro-combustion physics. Hence, development of a new cost-effective analyzing tool for micro-combustor system is essential to understand the details about the fluid dynamics, chemical kinetics and heat transfers occurring in micro-combustor, bridging the fundamental knowledge, experimental measurement and engineering design and optimization.

The past experimental works [2] have proved that it is impossible to propagate flames in a small gap around millimeter scale, which is known as quenching distance. The investigation indicates that there are two kinds of mechanisms, namely thermal quenching and radical quenching, leading to flame quenching in smaller dimension [3]. To develop a micro-combustor system, one of the most challenging tasks is to maintain stable combustion in a micro-scale combustion chamber, which is normally considered to be around the flame quenching distance in the traditional sense, to constantly convert the chemical energy to thermal energy. Some theoretical analysis of the combustion mechanism in simple micro-chambers has been performed [4] to show the feasibility of stable combustion in micro-combustor. The fundamental understanding of combustion mechanism in micro-scaled chambers, which is very essential to the design and optimization of power MEMS devices, is not understood well at present. Due to the difficulties in conducting spatially resolved measurements of combustion characteristics in micro-scale devices, the numerical simulation can be a cost-effective approach to study the micro-combustion mechanism. Norton and Vlachos [5] conducted two-dimensional CFD simulation to analysis the premixed methane/air flames stability in a micro-combustor, consisting of two parallel, infinitely wide plates of length of 1 cm and small distance. They studied the effects of micro-combustor dimension, conductivity and thickness of wall, external heat loss on combustion characteristics. Norton and Vlachos [6] reported the CFD study on the micro-combustion stability of

R. Kamali is with the Department of Mechanical Engineering, Shiraz University, Shiraz, Iran (e-mail: rkamali@shirazu.ac.ir).

propane/air mixture. Choi [7] performed the numerical simulation of hydrogen/air flame propagation near extinction condition in a micro-combustor. Spadaccini [8] studied the temperature distribution within combustion chamber with different inlet geometries using three-dimensional numerical simulation accounting the chemical kinetics hydrogen–air reaction mechanism.

In this paper, Computational Fluid Dynamics (CFD) - based numerical simulations are conducted to study the combustion of stoichiometric hydrogen–air in a number of micro-scaled cylindrical chambers. Detailed chemical reaction mechanism in combustion of hydrogen–air mixture is employed in the CFD simulations. In order to study the dimensional scaling effect on the combustion, the aspect ratio of the combustion chamber is kept the same in all simulations, while the chamber dimension, e.g. inlet diameter of chamber, is scaled down from millimeter level to micron level.

In this paper, the effects of chamber size, heat conduction within chamber wall, and heat loss through the wall on combustion characteristics in the chamber are investigated by numerical simulations. The simulation results indicate that stable combustion in a micro-scaled chamber can be achieved through balancing the flow residence time and the chemical reaction time and optimizing the thermal condition. Since the residence time will be shortened in a micro-combustion chamber, it is important to shorten chemical reaction time as well in order to ensure the completion of the combustion process. According to the chemical kinetics theory, one of the possible measures to shorten the chemical reaction time

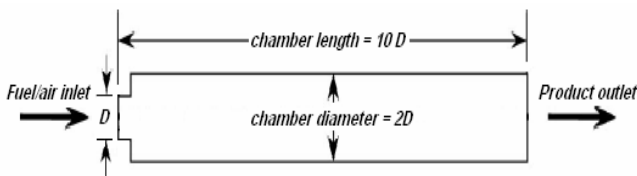


Fig. 1 Schematic diagram of the micro-scaled combustion chamber for micro-combustion modeling

is to increase the reaction rate by ensuring a high reaction temperature. This in turn can be achieved by reducing the heat loss from the combustion chamber.

The specific objectives of the paper are to:

- ◆ Identify the appropriate governing equations for the problem.
- ◆ Develop a computer code to:
  - o Create a computational grid.
  - o Solve the governing equations on the computational domain.
- ◆ Compare the predictions of the numerical simulation.
- ◆ Make suggestions for the better performance of the device.

## II. COMPUTATIONAL MODEL

### A. Model Geometry and the Mesh

The geometry of the cylindrical chamber used in this study is shown in Fig. 1. The effects of chamber dimension and wall treatment on combustion characteristics are studied through scaling down the cylindrical chamber from a relatively large scale to a micro-scale while keeping the same shape aspect ratio. The inlet diameter ( $D$ ) of the chamber is varied from the large size to the small size at 0.5, 0.2, 0.08, and 0.045 mm, respectively. The ratio of chamber diameter to inlet diameter ( $D$ ) is maintained at 2. The ratio of chamber length ( $L$ ) to inlet diameter ( $D$ ) is fixed to be 10. Stoichiometric hydrogen–air mixture is injected into the cylindrical chamber from the inlet located at one axial end with a step expansion as shown in Fig. 1. Because of the axial symmetry of the combustion chamber, the geometry is modeled as a two-dimensional axis-symmetric model. For the all cases analyzed in this study, a structured grid is used to mesh the models for the CFD simulations as shown in Fig. 2. The whole computational domain including both combustion chamber and inlet throttle is meshed using about 24375 cells. This fine mesh size will be able to provide good spatial resolution for the distribution of most variables within the combustion chamber.

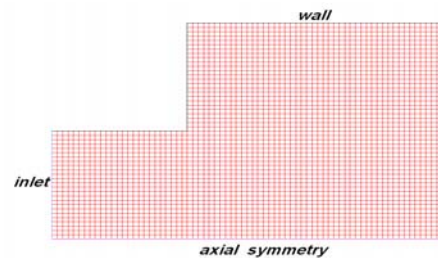


Fig. 2 Numerical grid of the computational domain at inlet

### B. Fluid Flow Modeling

The characteristic length of the combustion chamber and the reacting gas flow path in micro-combustors, even for MEMS systems, is still sufficiently larger than the molecular mean-free path (average distance between two successive collisions of a molecule) of the air and other gases flowing through the systems. Hence, the fluid media can be reasonably considered as continuum in this study. The Navier–Stokes equation is solved using Eulerian mixture model for the fluid domain and no-slip condition on the wall is applied.

### C. Governing Equations

A computer code is used to perform numerical simulations of the fluid flow in combustion chamber by solving the conservation equations of mass, momentum, energy and species.

Continuity Equation:

$$\frac{\partial \rho}{\partial t} + \frac{\partial}{\partial x_i} (\rho u_i) = 0 \quad (1)$$

Momentum Equation:

$$\frac{\partial}{\partial t}(\rho u_i) + \frac{\partial}{\partial x_j}(\rho u_i u_j) = -\frac{\partial p}{\partial x_i} + \frac{\partial \tau_{ij}}{\partial x_j} \quad (2)$$

where  $p$  is the static pressure and the stress tensor  $\tau_{ij}$  is given by:

$$\tau_{ij} = \mu \left( \frac{\partial u_i}{\partial x_j} + \frac{\partial u_j}{\partial x_i} \right) - \frac{2}{3} \mu \delta_{ij} \text{div} V \quad (3)$$

where  $\mu$  is the molecular viscosity and the second term on the right hand side is the effect of volume dilation.

Energy Equation:

$$\begin{aligned} \frac{\partial}{\partial t}(\rho E) + \frac{\partial}{\partial x_i}(u_i(\rho E + p)) = \\ \frac{\partial}{\partial x_i} \left( k_{eff} \frac{\partial T}{\partial x_i} - \sum_j h_j J_j + u_j (\tau_{ij})_{eff} \right) + S_h \end{aligned} \quad (4)$$

where  $k_{eff}$  is the effective conductivity and  $J_j$  is the diffusion flux of species  $j$ . The first three terms on the right-hand side of Equation represent energy transfer due to conduction, species diffusion, and viscous dissipation, respectively.  $S_h$  includes the heat of chemical reaction, and any other volumetric heat sources we have defined.

In equation (4),

$$E = h - \frac{P}{\rho} + \frac{u_i^2}{2} \quad (5)$$

where sensible enthalpy  $h$  is defined for ideal gases as

$$h = \sum_j m_j h_j \quad (6)$$

Where  $m_j$  is the mass fraction of species  $j$  and

$$h_j = \int_{T_{ref}}^T c_{p,j} dT \quad (7)$$

where  $T_{ref}$  is 298.15 K.

Species Conservation Equation:

When we choose to solve conservation equations for chemical species, we predict the local mass fraction of each species,  $m_i$ , through the solution of a convection-diffusion equation for the  $i$ th species. This conservation equation takes the following general form:

$$\frac{\partial}{\partial t}(\rho m_i) + \frac{\partial}{\partial x_i}(\rho u_i m_i) = -\frac{\partial}{\partial x_i} J_{i,i} + R_i + S_i \quad (8)$$

where  $R_i$  is the net rate of production of species  $i$  by chemical reaction and  $S_i$  is the rate of creation by addition from the dispersed phase. An equation of this form will be solved for  $N-1$  species where  $N$  is the total number of fluid

phase chemical species present in the system. Since the mass fraction of the species must sum to unity, the  $N$ th mass fraction is determined as one minus the sum of the  $N-1$  solved mass fractions. To minimize numerical error, the  $N$ th species should be selected as that species with the overall largest mass fraction, such as  $N_2$  when the oxidizer is air.  $J_{i,i}$  is the diffusion flux of species  $i$ , which arises due to concentration gradients. We use the dilute approximation, under which the diffusion flux can be written as

$$J_{i,i} = -\rho D_{i,m} \frac{\partial m_i}{\partial x_i} \quad (9)$$

Here  $D_{i,m}$  is the diffusion coefficient for species  $i$  in the mixture.

The reaction rates that appear as source terms in Equation (8) are computed by Laminar finite-rate model that effect of turbulent fluctuations are ignored, and reaction rates are determined by Arrhenius expressions. The net source of chemical species  $i$  due to reaction  $R_i$  is computed as the sum of the Arrhenius reaction sources over the  $N_R$  reactions that the species participate in:

$$R_i = M_i \sum_{k=1}^{N_R} \hat{R}_{i,k} \quad (10)$$

where  $M_i$  is the molecular weight of species  $i$  and  $\hat{R}_{i,k}$  is the Arrhenius molar rate of creation/destruction of species  $i$  in reaction  $r$ .

#### D. Boundary Conditions

A fixed composition (a stoichiometric mixture) of hydrogen-air is specified at the fuel inlet of micro-combustion chamber. The inlet temperature of fuel mixture is considered to be uniform at 300 K. A fixed, uniform velocity 5 m/s is specified at the inlet. As the combustion chamber diameter is about twice of the diameter inlet of fuel/air mixture. Hence, the cross-section area of the combustion chamber will be about four times of the inlet area. The averaged velocity of gas mixture at the chamber cross section will be about 1.25 m/s before it is burnt. Since the averaged gas mixture velocity of 1.25 m/s is lower than the flame speed, it will help the flame stable in the combustion chamber. Axi-symmetric boundary conditions are applied along the central axis of the combustion chamber. At the exit, a pressure outlet boundary condition is specified with a fixed pressure of  $1.013 \times 10^5$  Pa. At the chamber wall, no-slip boundary condition and no species flux normal to the wall surface are applied.

The thermal boundary conditions on the chamber wall relate to two main heat transfer factors: heat loss through the chamber wall to the ambient and heat conduction within the wall. For the condition of heat loss through chamber wall, two kinds of heat loss conditions are assumed in this study: adiabatic wall condition and fixed effective heat transfer coefficient condition. For the latter case, the heat loss through wall can be expressed as

$$q = h(T_{wall} - T_a) \quad (11)$$

where  $h$  is the effective heat transfer coefficient;  $T_{wall}$  is the temperature on the wall;  $T_a$  is the ambient temperature.

Hence, the heat loss through the wall can be characterized by specifying the effective heat transfer coefficient. As for the heat conduction in the chamber wall, the wall thickness is firstly ignored to decouple its interaction with the heat loss through chamber wall. Hence, we can highlight the effect of heat loss through chamber wall on the combustion while downscaling the combustion chamber size. The previous works (Norton and Vlachos [5,6]; Ronney, [9]) illustrated that the heat conduction within the chamber wall might have significant effect on the combustion behavior depending upon wall properties such as wall dimension and thermal conductivity. Therefore, the effect of heat conduction within the combustion chamber wall on combustion characteristics is investigated by explicitly modeling the wall thickness in some later study cases. Here the wall thickness is assumed to be the same as the inlet radius of the chamber, which is the common design for micro-scaled devices. In this study, three different wall materials with relatively large differences in heat conductivity are selected to study the effect of wall heat conductivity on combustion behavior in the chamber. Three kinds of wall material are the materials with (1) high heat conductivity material such as metal, silicon; (2) medium heat conductivity such as ceramics; and (3) low heat conductivity material such as insulation material.

#### E. Numerical Model

A segregated solution solver is used to solve the above-mentioned set of governing equations. Since the Reynolds number of the fluid flow ranges from about 11 when  $D=0.045\text{mm}$  to 126 when  $D=0.4\text{mm}$  for the simulated cases, laminar viscous flow is considered. The fluid density is calculated using the ideal gas law. The fluid mixture specific heat, viscosity, and thermal conductivity are calculated from a mass fraction weighted average of species properties. The CFD simulation convergence is judged upon the residuals of all governing equations. This "scaled" residual is defined as:

$$R^\phi = \frac{\sum_{cells} p \left| \sum_{nb} a_{nb} \phi_{nb} + b - a_p \phi_p \right|}{\sum_{cells} p \left| a_p \phi_p \right|} \quad (12)$$

where  $\phi_p$  is a general variable at a cell  $p$ ,  $a_p$  is the center coefficient,  $a_{nb}$  are the influence coefficients for the neighboring cells, and  $b$  is the contribution of the constant part of the source term. The results reported in this paper are achieved when the residuals are smaller than  $1.0 \times 10^{-6}$ .

The combustion model is validated by simulating the combustion of premixed hydrogen-air under adiabatic condition and comparing with the measurement of adiabatic flame reported by Glassman [3]. The comparisons of flame temperature and mole fraction of species obtained from the model prediction and experiment are listed in Table I. The numerical predictions are in reasonable agreement with the

experimental data.

### III. RESULTS AND DISCUSSION

A number of numerical simulations have been performed to study the combustion phenomena when the combustion chamber size is reduced from a relatively large scale to a micro-scale under different wall condition.

#### A. Combustion in the Micro-Scaled Chambers under Adiabatic Wall Condition

Fig. 3 shows the predicted temperature contours on the cross section of combustion chambers for different inlet diameters:

TABLE I COMPARISON OF MOLE FRACTION OF SPECIES IN STOICHIOMETRIC HYDROGEN-AIR MIXTURES IN SIMULATION AND EXPERIMENT		
Mole fractions	Experimental results (Glassman, 1996)	Numerical results
$H_2O$	0.323	0.335
$O_2$	0.005	0.008
$H_2$	0.015	0.011
$N_2$	0.644	0.644
$NO$	0.003	0.002

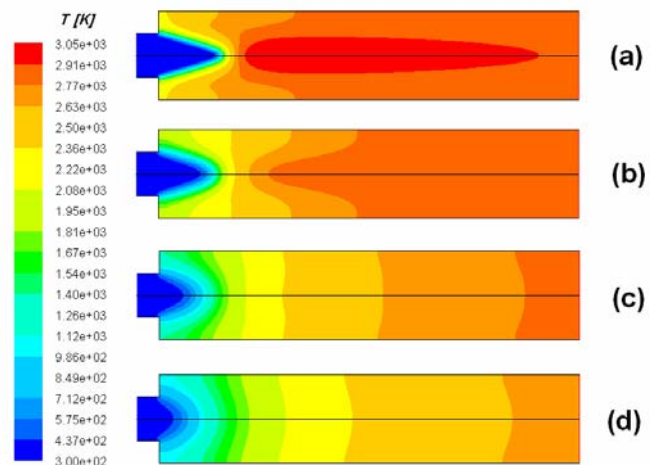


Fig. 3 Contours of temperature [K] on the cross section along central axis of various sized combustion chambers with the inlet diameter of: (a) 0.5 mm; (b) 0.2 mm; (c) 0.08 mm; (d) 0.045 mm under adiabatic wall condition

(a) 0.5 mm, (b) 0.2 mm, (c) 0.08 mm and (d) 0.045 mm, under adiabatic wall condition. For the same simulation cases, the contours of Arrhenius rate of reaction, which is regarded as an indicator of global chemical reaction rate, are shown in Fig. 3. The combustion chamber dimensions shown in these contour plot figures are normalized by the corresponding inlet diameter ( $D$ ) for each simulation case. In this way, the relative position of combustion zone and physical property distribution in the different-sized combustion chambers can be easily compared.

It can be seen from Figs. 3 and 4 that the combustion can be self-sustained in the micro-scaled combustion chamber if

the wall is maintained as adiabatic. The gas temperature is raised significantly due to the heat released from combustion. The highest temperature is obtained at the exit of combustion chamber at a range of 2600–3000 K. The flame temperature can be as high as 3000K for the largest combustor in this study, which is almost the same as the adiabatic flame temperature of the combustion of stoichiometric hydrogen–air mixture. As the combustion chamber size decreases, the exit temperature of the combustion product decreases as well. However, as the combustion chamber size decreases, the ratio of the combustion zone to chamber volume increases significantly as shown in Fig. 3.

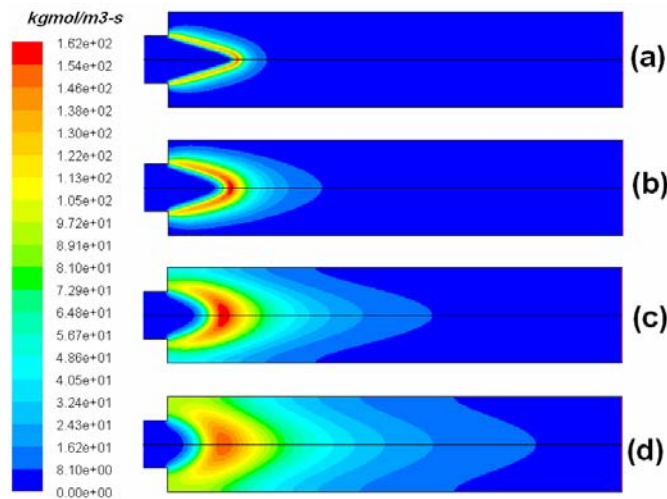


Fig. 4 Contours of production rate [kgmol/m<sup>3</sup>-s] of water at the cross section along the central axis of various sized combustion chambers with the inlet diameter of: (a) 0.5 mm; (b) 0.2 mm; (c) 0.08 mm; (d) 0.045mm under adiabatic wall condition

Fig. 5 show the gas temperature along the central axis of the chamber, respectively. Here, the dimensionless axial distance is defined as the ratio of the axial distance to the inlet diameter. When the chamber dimension is large enough, the gas mixture has enough residence time in the chamber, so that combustion will be completed before it flows out of the combustion chamber. With the completed combustion in the large chambers, the gas product flows out of the combustion chamber almost at adiabatic flame temperature 3000K as shown in Fig. 5. However, when combustion chamber size decreases, the chemical reaction mechanism is kept same. The reaction zone may occupy more and more space of the temperature micro-combustion chamber. Fig. 5 also indicates the temperature of the combustion gas product decreases as the combustion chamber size decreases due to the incomplete combustion in smaller chambers. The simulation results under the adiabatic wall condition indicate that the decreasing of combustion chamber size does not have significant effect on the global chemical reaction rate within the chamber. But, decreasing the combustion chamber size may limit the combustion efficiency. This is due to the fact that the gas mixture does not have enough residence time to finish the chemical reaction completely in the smaller chambers. Hence, to obtain a stable combustion in a micro chamber, the chamber

dimension should be larger than the adiabatic flame thickness at least.

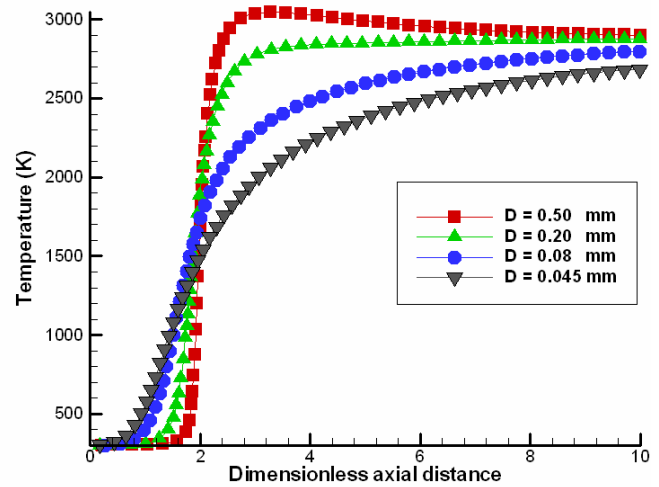


Fig. 5 Gas temperature [K] distribution along the central axis for the scaled chambers of various inlet diameters ( $D$ ) under adiabatic wall condition

#### B. Combustion in the Micro-Scaled Chambers under Heat Loss through Wall Condition

In reality, it is almost impossible to achieve adiabatic condition at the combustion chamber walls. Certain amount of heat loss through the combustion chamber wall cannot be avoided. If the characteristic length of a combustion chamber is  $D$ , then the chamber wall surface area  $S$  can be expressed as  $S \propto D^2$ , and the chamber volume  $V$  as  $V \propto D^3$ . Then the ratio ( $R$ ) of heat loss through the wall to the combustion heat generated in the chamber volume can be expressed as:

$$R = \frac{hS\Delta T}{VR_c\Delta H} \propto \frac{h\Delta T}{R_c\Delta HD} \quad (13)$$

where  $h$  is the effective heat transfer coefficient,  $R_c$  is volumetric chemical reaction rate,  $\Delta H$  is the combustion heat,  $\Delta T$  is the temperature difference between the inside of combustion chamber and the ambient. Hence, it is clear that the ratio of heat loss through wall to total heat generation from combustion may increase significantly as the chamber characteristic dimension ( $D$ ) decreases. If this ratio is too high, the self-sustained combustion will become impossible, and could lead to thermal quenching in the micro-scale combustion process.

Fig. 6 shows the predicted temperature distributions within the combustion chambers for different inlet diameters of (a) 0.5 mm; (b) 0.2mm and (c) 0.08mm under the heat loss through wall condition, respectively. The heat loss condition is applied by specifying a constant heat transfer coefficient on the chamber wall, as defined in Eq.(11). Here, the constant effective heat transfer coefficient is assumed to be 100W/m<sup>2</sup>/K [1]. The distributions of water production rate for these simulation cases are shown in Fig. 7.

It can be clearly seen from Fig. 8 that, compared with the case of adiabatic condition, the flame structure changes to

cone shape when there is heat loss through wall. The flame core in the downstream from the inlet has the highest gas temperature and the value is about 1900 K. Fig. 8 shows the gas temperature distribution along the chamber axis. Due to the heat loss through the chamber wall, the temperature of combustion gas-product decreases as they flow downstream and exit the chamber at a lower temperature. As the dimension of the combustion chamber decreases, the ratio of heat loss to the total combustion heat increases rapidly. As a result, the temperature of the flame core decreases with decreasing combustion chamber size. When the same heat loss condition is applied to the smallest combustion chamber (with an inlet diameter of 0.045 mm) in this study, the combustion cannot sustain in the chamber.

An important consequence of the decreased flame core temperature is that the chemical reaction rate of combustion will be lowered as well. This can be clearly seen by comparing the water production rate distributions for the case under the heat loss through wall condition (as shown in Fig. 7) with those under adiabatic wall condition (as shown in Fig. 4). In addition, the effect of heat loss through wall on lowering the chemical reaction rate becomes more significant when the chamber size is smaller.

The dimensional analysis from Eq. (2) also indicates that the heat loss through the wall has significant effect on the combustion behavior in micro-scaled chambers. As the combustion chamber size decreases, the ratio of surface area to volume increases. This will lead to a higher percentage of the combustion heat to be lost through the wall. This also implies that only the rest smaller percentage of the combustion heat is available to sustain the combustion. When the combustion temperature is lowered, it leads to lower chemical reaction rate as well as total heat generation rate. This mechanism may ultimately lead to the thermal quenching effect in the micro-combustion chamber when the dimension is too small or when the heat transfer coefficient is too high. Hence, to maintain the stable combustion within a micro-combustor, the heat loss through wall should be controlled properly.

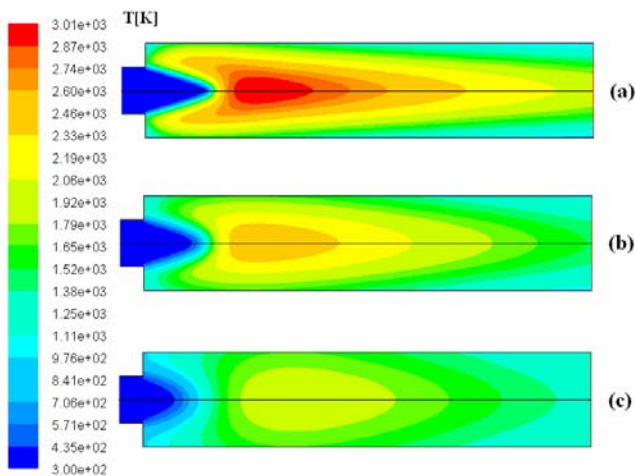


Fig. 6 Contours of temperature [K] on the cross section along the central axis of various sized chambers with the inlet diameters of (a) 0.5 mm; (b) 0.2 mm; (c) 0.08 mm under the heat loss through wall condition

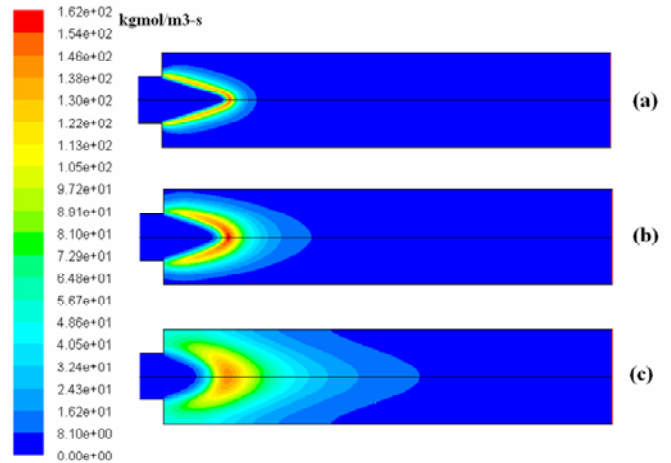


Fig. 7 Contours of water production rate [kmol/m<sup>3</sup>/s] on the cross section along the central axis of various sized chambers with the inlet diameters of (a) 0.4 mm; (b) 0.2 mm; (c) 0.1 mm under the heat loss through wall condition

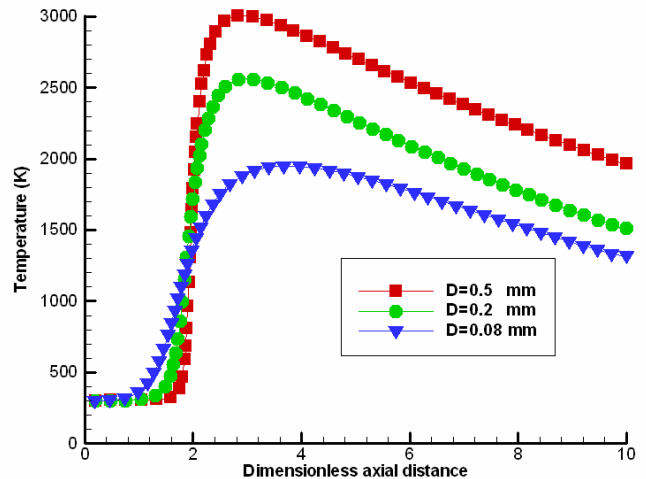


Fig. 8 Temperature distributions [K] along the central axis for the scaled chambers of various inlet diameters ( $D$ ) with heat loss through wall

### C. Combustion in Micro-Chambers with Different Wall Heat Conductivity

In this section, the effect of heat conduction within chamber wall on combustion characteristics in micro-scaled combustion chamber is studied. In this case the inlet diameter of chamber is selected to be 0.2mm and the wall thickness is the same as the inlet radius equal to 0.1 mm. Three kinds of wall materials are selected to study the effect of heat conduction on the combustion. First, high heat conductive material such as metal and silicon is selected. It has relatively high heat conductivity around 200W/m/K. Second, medium heat conductive material such as ceramic is chosen. Its heat conductivity is about 10W/m/K. And, the third kind of the selected material has lower heat conductivity at the level of 0.5W/m/K such as insulation material. As for the heat loss to the ambient, we choose a fixed effective heat transfer

coefficient of  $50\text{W/m}^2\text{K}$  on the chamber wall. Fig. 9 shows the temperature contours at the cross section of combustor for different cases: (a) high heat conductive wall, (b) medium heat conductive wall, and (c) low heat conductive wall.

It can be obviously seen from Fig. 9 that when the wall thermal conductivity decreases, the maximum temperature in the flame core increases and the flame core (high temperature zone) shifts slightly toward the downstream away from the inlet. This indicates that the heat conduction in the chamber wall has two competing effects on the overall combustion behavior. On the one hand, the axial heat conduction in the chamber wall provides a route for the heat transfer from the post combustion region to the unburned upstream region. This will help to pre-heat the incoming gas reactants and enhance the ignition and flame stability. On the other hand, the radial heat conduction in the chamber wall allows the exterior heat loss to the environment. This will induce the energy loss from the combustion system lowering the flame temperature, which can delay the flame ignition and even result in flame extinction. The distributions of water production rate shown in Fig. 10 also help in proving the competing effects of heat conduction in the chamber wall on the overall combustion in the chamber. The highest water production rate in the combustion reaction zone comes when the chamber wall has medium heat conductivity. In addition, the temperature distribution in the chamber wall also has significant effects on the material stress, which is important to the combustor performance. The wall temperature distributions along the axial direction under various levels of wall heat conductivity are shown in Fig. 10. When the wall has a lower thermal conductivity, there will exist a high-temperature gradient in the wall and the hot spot nearby the flame-core. This will create stringent requirements on the wall material to allow such high flame temperature and temperature gradient (resulting in high thermal stress). In contrast, if the wall has a higher thermal conductivity, the wall temperature will have more uniform distribution. The reduced thermal gradients will also reduce thermal stresses in the chamber wall.

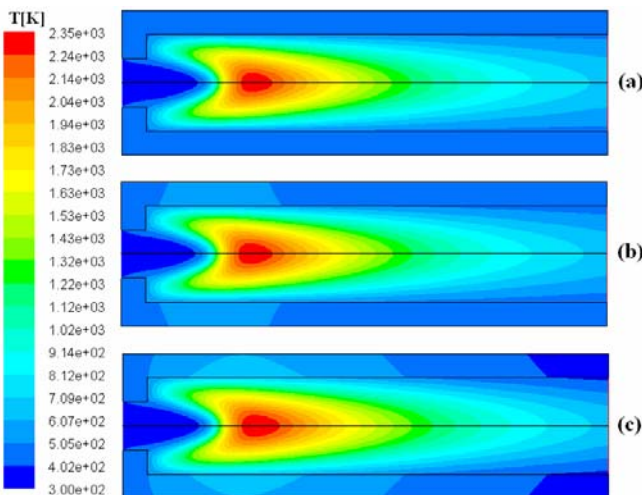


Fig. 9 Contours of temperature [K] on the cross section along the central axis of the combustion chamber with different wall heat conductivity of (a)  $200\text{W/mK}$ ; (b)  $10\text{W/mK}$ ; (c)  $0.5\text{W/mK}$

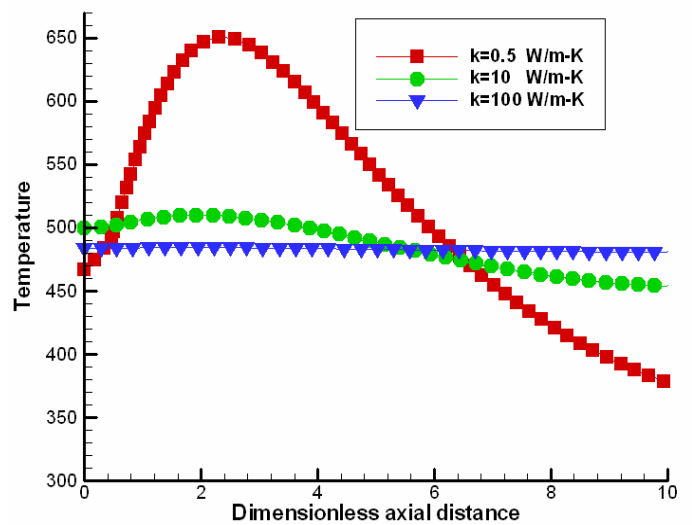


Fig. 10 Temperature distributions [K] along the outer wall of the combustion chamber with different wall heat conductivity

#### IV. CONCLUSION

In the present work, a computer code has been developed to study the combustion phenomena of the hydrogen–air mixture in a series of combustion chambers when the inlet diameter is reduced from a relatively large size of  $0.5\text{mm}$  to a micro-scale size of  $0.045\text{mm}$ . The simulations also include the effects of different thermal conditions on the chamber wall by taking into account the heat loss through the wall and heat conduction within the wall. The prepared algorithm and the computer code are capable of modeling mixture effects in different fluid flows including chemical reactions, viscous and mass diffusion effects.

Theoretically, stable combustion can only occur in a combustion chamber when the reactant residence time is larger than the chemical reaction time. For the case of combustion in traditional large-scale combustors, the residence time for reactant in the combustion chamber is always large enough for complete combustion. Decreasing the dimension of combustion chamber leads to significant reduction in residence time as the reactant flow speed cannot reduce accordingly. This is because a certain flow rate of reactant needs to be maintained to achieve the requirement of power generation rate. But, the chemical reaction time is remained as usual. The direct consequence of insufficient residence time in micro-combustion chamber is that the combustion may not be complete within the combustor. Lower combustion efficiency may lead to insufficient heat generation to maintain self-sustained combustion, and further result in quenching. The numerical simulation of combustion of premixed hydrogen–air in micro-scaled chamber with adiabatic wall condition proves that the combustion may be stable only when the combustion chamber size is large enough comparing to the adiabatic flame thickness.

In the traditional large-scale combustor, the heat loss through wall only takes a small part of total combustion heat generated within the chamber. Hence, many traditional large-

scale combustors can work with high thermal efficiency. However, as the combustion chamber dimension decreases, the ratio of surface area to volume increases. In a micro-scaled combustion chamber, heat losses through the wall may take significant percentage of the total combustion heat generation within the chamber volume and results in significantly lower chemical reaction temperature and volumetric chemical reaction rate. In this case, the chemical reaction time may increase. Hence, quenching may occur in the micro-combustion chamber when the dimension is too small or the heat transfer coefficient at the outer wall is too high.

Heat conduction in the chamber wall also plays an important role in the performance of micro-combustor. Lower wall heat conductivity can reduce the heat loss from the system and stable the combustion. But, it may also cause hot spot on the wall near the flame and high-temperature gradient in the wall, which post high requirement on the wall material. On the contrary, the higher heat conductivity can produce relatively even wall temperature distribution that is good to wall material, and higher heat loss that should be managed properly to stabilize the micro-combustion system.

Through numerical simulation of combustion of hydrogen–air mixture in micro-scaled chambers, it can be concluded that the numerical model is able to capture the basic micro-combustion mechanism. The quenching phenomena and mechanism in micro-combustion have been explored and discussed. Stable combustion in the micro-combustor is achievable by system optimization of the combustor geometry, thermal conditions and reacting flow dynamics. The numerical modeling approach presented in this paper is helpful in the design and optimization of combustion-based micro-power generation device.

#### REFERENCES

- [1] Carlos Fernandez-Pello, A., 2002. Micro-power generation using combustion: issues and approaches. Twenty-Ninth International Symposium on Combustion, Sapporo, Japan, the Combustion Institute
- [2] Ono, S., Wakuri, Y., 1977. An experimental study on the quenching of flame by narrow cylindrical passage. Bulletin of JSME 20 (147)
- [3] Glassman, I., 1996. Combustion. Academic Press, California.
- [4] Lee, D.H., Kwon, S., 2002. Heat transfer and quenching analysis of combustion in a micro combustion vessel. Journal of Micromechanics and Micro engineering 12, 670–676.
- [5] Norton, D.G., Vlachos, D.G., 2003. Combustion characteristics and flame stability at the micro-scale: a CFD study of premixed methane/air mixtures. Chemical Engineering Science 58, 4871–4882.
- [6] Norton, D.G., Vlachos, D.G., 2004. A CFD study for propane/air micro-flame stability. Combust. Flame 138, 97–107.
- [7] Choi, K.H., Na, H.B., Lee, D.H., Kwon, S., 2004. Numerical simulation of flame propagation near extinction condition in a micro-combustor. Micro-scale Thermophysical Engineering 8, 71–89.
- [8] Spadaccini, C.M., Mehra, A., Lee, J., Zhang, X., Lukachko, S., Waitz, A.I., 2003. High power density silicon combustion system for micro gas turbine engines. Journal of Engineering for Gas Turbines and Power 125, 709–719.
- [9] Ronney, P.D., 2003. Analysis of non-adiabatic heat-recirculating combustors. Combust. Flame 135 (4), 421.